

**Ryzhkov Sergiy**DSc (Eng.), professor, <https://orcid.org/0000-0001-9560-2765>

Yancheng Polytechnic College,

International Academy of Marine Science, Technology and Innovation, Yancheng, China

**Chengjian Dong**<https://orcid.org/0000-0003-3529-6529>

School of Automobile and Transportation, Yancheng Polytechnic College, Yancheng, China

**RESEARCH OF GAS DYNAMICS OF HIGHLY EFFICIENT TURBO-IMPACT COMPRESSED GAS SEPARATOR FOR GAS TURBINE INSTALLATION**

**Abstract.** *The gas dynamics of multiphase mixtures of high-pressure fuels in turboimpact separators with coagulation structural elements at a flow rate of the working medium  $G = 500-2200$  kg/h were investigated. The geometry of the turboimpact separator with a radial guide jet element consists of a first stage and a separator, consists of a plate with a diameter of 250 mm, on a diameter of 97 mm of which there is a corrugated separation element, the dimensions of which vary from 10 to 40 mm, depending on the working geometry. At the bottom of the first stage of the separator are grooves of rectangular shape  $3 \times 2$  mm at a distance of 27 mm. In the second stage of the separator at a diameter of 270, 240 and 180 mm respectively there are through rectangular grooves  $5 \times 10$  mm. In a turboimpact separator with a radial coagulation element, a uniform velocity distribution was observed, the maximum of which is 43.7 m/s, which indicates a uniform turboimpact particle transfer. The turboimpact separator with a radial guide jet element is characterized by the close location of the corrugated mesh element to the jet cleaning zone. Prevalence of flow, in the channel near grid element forms a vortex zones, which will further lead to the displacement of undeposited particles to the lower wall of the channel. In the first stage of purification turboimpact separator with radial coagulation element after passing through the working medium of the jet cleaning zone, the flow was evenly distributed throughout the entire section of the channel, which contributes to the uniform distribution of the polydisperse phase in the working medium in front of the mesh element. It was established that the optimal pressure drop of 1 KPa is observed in a turboimpact separator with a radial arrangement of a coagulation element, which allows using this design for cleaning multiphase mixtures of high-pressure fuels.*

**Keywords:** *turboimpact transfer; separator; particle deposition; gas dynamics; multiphase mixtures; high-pressure fuels*

### **The formulation of the problem, its connection with current scientific and practical tasks**

Modern power plants require the use of high-quality multiphase mixtures of high-pressure fuels. The content of liquid and solid phases significantly reduces the service life, degrades the performance characteristics and increases the operating costs of power plants. Research and development of separation equipment makes it possible to improve the quality of multiphase mixtures of high-pressure fuels based on the transport and polypersemedium under the combined action of inertia forces, turbophoresis, diffusio-phoretic forces, resistance for a unit mass of the particle and Saffman forces. The design and development of separation equipment should take into account the main mechanisms of turboimpact transfer intensification, capable of purifying multiphase mixtures of high-pressure fuels above 99.8%.

### **Analysis of recent research and publications in which the solution of this problem**

Significant success in the development and creation of separation equipment was achieved by companies of German, Spanish and American production, namely Selton, Pall Corporation, Parker Zander, Contec and Gora. The German company Selton manufactures separation filters that have a metal structure that provides a slight pressure drop (from 0.6 MPa) and high filtration fineness (at 0.1 microns droplet size up to 99.99%). In turn, the American company Pall Corporation manufactures separation equipment with removable filters (SeptraSol, SeptraSol, Pall, Plus), filtration fineness (at 0.3 microns, droplet size up to 99.99%). Parker Zander produces a series of separation equipment brand Ecosep with removable filters, the filtration fineness of which is at 0.01 microns from 92 to 99%.



At the bottom of the first stage of the separator are grooves of rectangular shape 3x2 mm at a distance of 27 mm. In the second stage of the separator at a diameter of 270, 240 and 180 mm respectively there are through rectangular grooves 5x10 mm.

To study the separator, a grid is constructed in the Cartesian coordinate system using triangular segments, which is constructed in accordance with the working geometry of the separator, the area of which does not exceed  $S = 25 \cdot 10^{-8} \text{ m}^2$ . In pic. Fig. 2 presents tetrahedral design grids of the separators under study. The design grids are built in the *Ansys Workbench batch* module without simplifying the designs. In places where the geometric parameters of the turboimpact separation element are reduced, local thickening of the grid consisting of smaller elements (from 120 thousand design elements, depending on the design solution) was performed.

Investigation of gas dynamics of turboimpact separators of multiphase mixtures of high-pressure fuels, purification of polydisperse medium, a mathematical model of the process of transfer of a multiphase medium of a turbo-impact separator consists of equations of gas dynamics of the process.

The gas dynamics equations of the process are based on the Navier-Stokes equations (1) and the continuity equation (2):

$$\frac{\partial}{\partial x_j} \left( \mu_{eff} \frac{\partial u_i}{\partial x_j} \right) = \frac{1}{\rho} \frac{\partial p}{\partial x_i} + \frac{\partial u_i u_j}{\partial x_j} \quad (1)$$

$$\frac{\partial u_i}{\partial x_j} = 0, \quad (2)$$

where  $u_i$  – velocity vector components;  $u_i u_j$  – double speed correlation;  $i, j = 1, 2$  and the Reynolds stress model (RSM) model as accurately simulates the effects caused by flow curvature, vortex, flow rotation, rapid changes in flow strength. The Reynolds stress equations are written as:

$$\frac{\partial}{\partial t} (\overline{\rho u'_i u'_j}) + C_{ij} = D_{T,ij} + D_{L,ij} + P_{ij} + G_{ij} + \phi_{ij} - \epsilon_{ij} + F_{ij} + S_{user}, \quad (3)$$

where  $\frac{\partial}{\partial t} (\overline{\rho u'_i u'_j})$  is the partial time derivative;

$C_{ij}$  – convective component;

$D_{T,ij}$  – turbulent diffusion;

$P_{ij}$  – formation of tension;

$G_{ij}$  – formation of buoyancy force;

$\phi_{ij}$  – pressure stress;

$\epsilon_{ij}$  – dissipation;

$F_{ij}$  – formation rotation of the system;

$S_{user}$  – member, specified by the user.

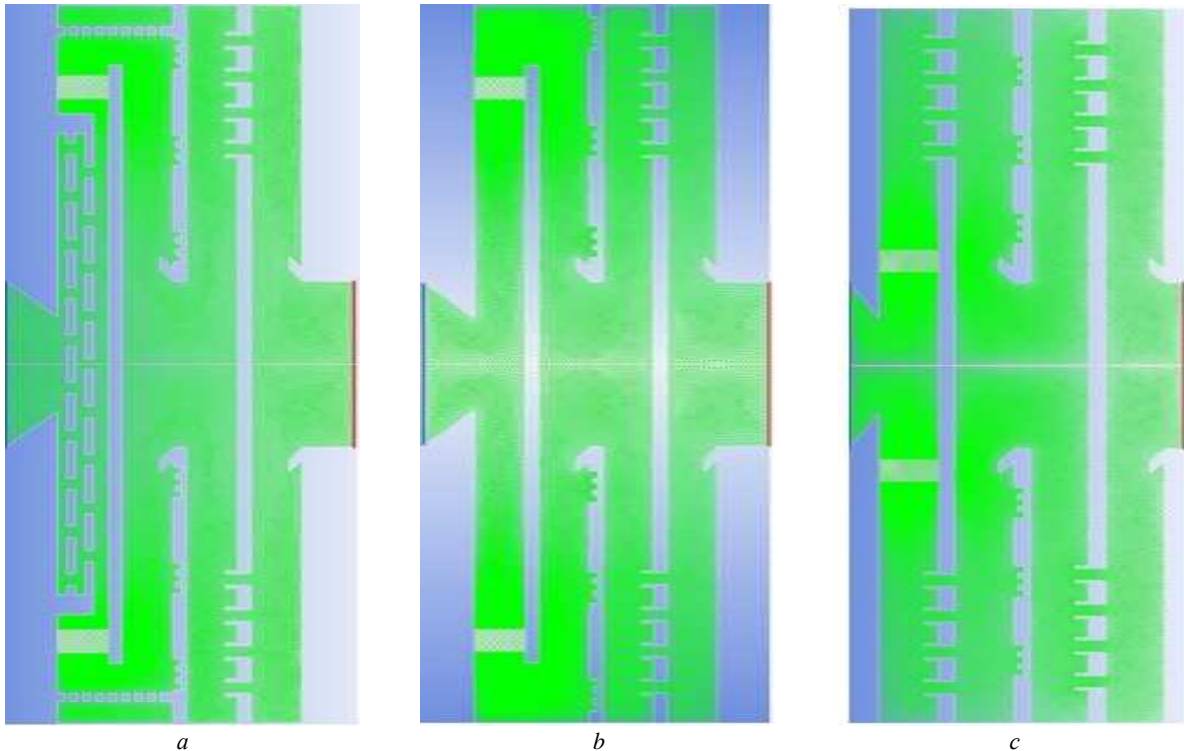


Figure 2 – Calculated grids of turboimpact separators: a – with a combined coagulation element; b – with a radial coagulation element; c – with a radial guide jet element

All the above terms in the strict formulation of the equation are determined by the formulas,  $C_{ij}$ ,  $D_{T,ij}$ ,  $P_{ij}$ ,

$G_{ij}$ ,  $\varphi_{ij}$ ,  $\varepsilon_{ij}$ ,  $F_{ij}$ ,  $S_{user}$ :

$$C_{ij} \equiv \frac{\partial}{\partial x_k} (\rho u_k \overline{u'_i u'_j}). \quad (4)$$

$$D_{T,ij} \equiv -\frac{\partial}{\partial x_k} \left[ \overline{\rho u'_i u'_j u'_k} + p (\delta_{kj} \overline{u'_i} + \delta_{ik} \overline{u'_j}) \right]. \quad (5)$$

$$D_{L,ij} \equiv -\frac{\partial}{\partial x_k} \left[ \mu \frac{\partial}{\partial x_k} (\overline{u'_i u'_j}) \right]. \quad (6)$$

$$P_{ij} \equiv -\rho \left( \overline{u'_i u'_k} \frac{\partial u_j}{\partial x_k} + \overline{u'_j u'_k} \frac{\partial u_i}{\partial x_k} \right). \quad (7)$$

$$G_{ij} \equiv -\rho \beta (g_i \overline{u'_j \theta} + g_j \overline{u'_i \theta}). \quad (8)$$

$$\varphi_{ij} \equiv p \left( \frac{\partial \overline{u'_i}}{\partial x_j} + \frac{\partial \overline{u'_j}}{\partial x_i} \right). \quad (9)$$

$$\varepsilon_{ij} \equiv 2\mu \frac{\partial \overline{u'_i}}{\partial x_k} \frac{\partial \overline{u'_j}}{\partial x_k}. \quad (10)$$

$$F_{ij} \equiv -2\rho \Omega_k (\overline{u'_j u'_m} \varepsilon_{ikm} + \overline{u'_i u'_m} \varepsilon_{jkm}). \quad (11)$$

From the above expressions  $C_{ij}$ ,  $D_{L,ij}$ ,  $P_{ij}$ ,  $F_{ij}$ , are calculated directly, and  $D_{T,ij}$ ,  $G_{ij}$ ,  $\varphi_{ij}$ ,  $\varepsilon_{ij}$ , are modeled in a form that allows closing the equation.

$D_{T,ij}$  can be found using the generalized gradient-diffusion model of Daly and Harlow:

$$D_{T,ij} = C_s \frac{\partial}{\partial x_k} \left( \rho \frac{\overline{u'_k u'_\ell} \frac{\partial \overline{u'_i u'_j}}{\partial x_\ell}}{\varepsilon} \right). \quad (12)$$

This equation can be written as follows:

$$D_{T,ij} = \frac{\partial}{\partial x_k} \left( \frac{\mu_t}{\sigma_k} \frac{\partial \overline{u'_i u'_j}}{\partial x_k} \right). \quad (13)$$

### Research results

The gas-dynamic characteristics of the working medium with flow rate  $G = 500 - 2200$  kg/h are investigated. Figure 3 shows the separation of the velocity of y in turboimpact separator at  $G = 1000$  kg/h. In a turboimpact separator with a radial coagulation element, a uniform velocity distribution is observed, the maximum of which is 43.7 m / s, which indicates a uniform turboimpact particle transfer.

The turboimpact separator with a radial guide jet element is characterized by the close location of the corrugated mesh element to the jet cleaning zone. Prevalence of flow, in the channel formed by grid element forms a vortex zones, which will further lead to the displacement of undeposited particles to the lower wall of the channel. In the first stage of purification turboimpact separator with radial coagulation element after passing through the working medium of the jet cleaning zone, the flow is evenly distributed throughout the entire section of the channel, which contributes to the uniform distribution of the polydisperse phase in the working medium in front of the mesh element.

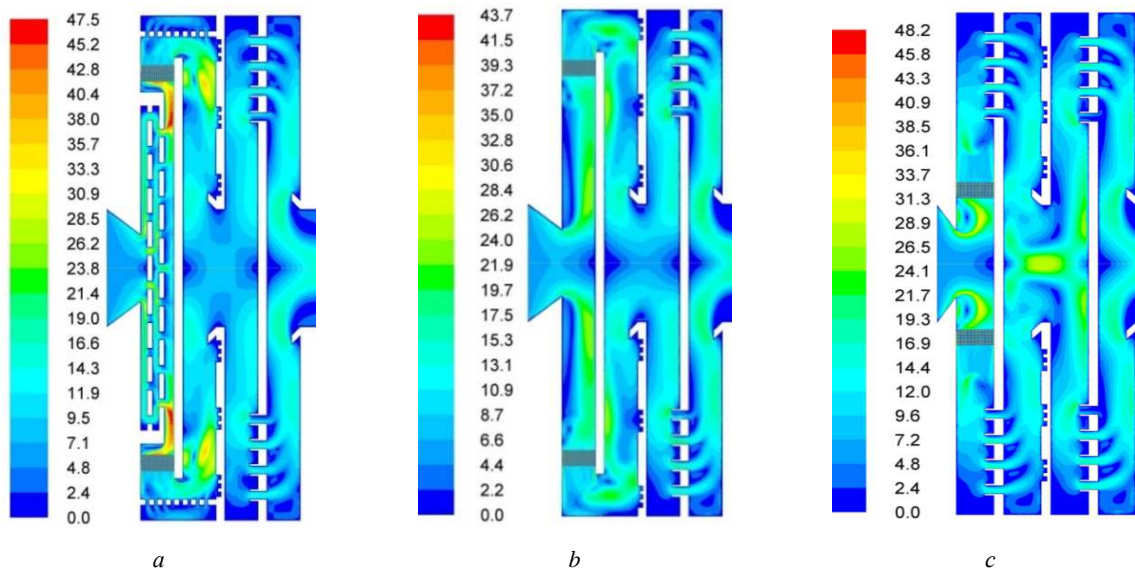


Figure 3 – Speed distribution in a turboimpact separator at  $G = 1000$  kg/h: a – with a combined coagulation element; b – with a radial coagulation element; c – with a radial guide jet element

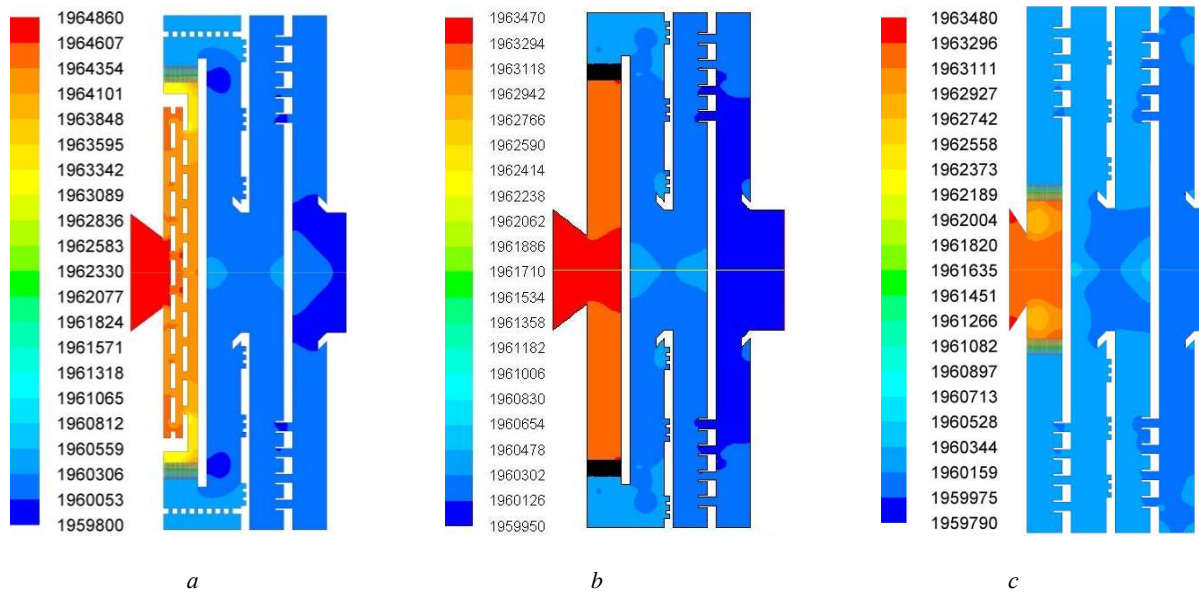


Figure 4 – Velocity distribution in turboimpact separator at  $G = 1000 \text{ kg/h}$ :  
 a – with a combined coagulation element; b – with a radial coagulation element; c – with a guide jet element

In design version 3, the working medium after passing through the mesh corrugated element enters the second section of the separation module through a 5 mm shea nozzle located in a circle. The results of calculations

of the flow part of the turboimpact separator for cleaning multiphase mixtures of high-pressure fuels from solid and liquid fractions are shown in Table 1–4.

Table 1 – Differential pressure in the separator channel (tothe instructional solution No1)

Section width, mm	Inlet Pressure of separator, Pa	Outflow Pressure of separator, Pa	Pressure drop of separator, Pa
<b>Fuel gas consumption 500 kg/h</b>			
10	1960000	1956563,2	3436,8
20	1960000	1958757,6	1242,4
40	1960000	1959308,2	691,8
<b>Fuel gas consumption 1000 kg/h</b>			
10	1960000	1946729,1	13270,9
20	1960000	1955214,5	4785,5
40	1960000	1958733,0	1267,0
<b>Fuel gas consumption 1500 kg/h</b>			
10	1960000	1929951,8	30048,2
20	1960000	1949533,0	10467,0
40	1960000	1956629,4	3370,6
<b>Fuel gas consumption 2200 kg/h</b>			
10	1960000	1930369,3	29630,7
20	1960000	1941247,7	18752,3
40	1960000	1954299,7	5700,3

Table 2 – Differential pressure in the separator channel (tothe instructional solution No2)

Section width, mm	Inlet Pressure of separator, Pa	Outflow Pressure of separator, Pa	Pressure drop of separator, Pa
<b>Fuel gas consumption 500 kg/h</b>			
10	1960000,0	1957886,2	2113,8
20	1960000,0	1959103,9	896,1
40	1960000,0	1959769,2	230,8

<b>Fuel gas consumption 1000 kg/h</b>			
10	1960000,0	1951701,0	8299,0
20	1960000,0	1956761,5	3238,5
40	1960000,0	1959243,0	757,0
<b>Fuel gas consumption 1500 kg/h</b>			
10	1960000,0	1941596,5	18403,5
20	1960000,0	1952850,7	7149,3
40	1960000,0	1958612,6	1387,4
<b>Fuel gas consumption 2200 kg/h</b>			
10	1960000,0	1927520,8	32479,2
20	1960000,0	1950459,2	9540,8
40	1960000,0	1957695,2	2304,8

Table 3 – Pressure drop in the separator channel (to the instructional solution No3)

Section width, mm	Inlet Pressure of separator, Pa	Outflow Pressure of separator, Pa	Pressure drop of separator, Pa
<b>Fuel gas consumption 500 kg/h</b>			
10	1960000,0	1956459,4	3540,6
20	1960000,0	1959589,0	411,0
40	1960000,0	1959653,2	346,8
<b>Fuel gas consumption 1000 kg/h</b>			
10	1960000,0	1946064,0	13936,0
20	1960000,0	1956731,1	3268,9
40	1960000,0	1958769,0	1231,0
<b>Fuel gas consumption 1500 kg/h</b>			
10	1960000,0	1928911,0	31089,0
20	1960000,0	1952600,4	7399,6
40	1960000,0	1957515,6	2484,4
<b>Fuel gas consumption 2200 kg/h</b>			
10	1960000,0	1904896,9	55103,1
20	1960000,0	1947115,7	12884,3
40	1960000,0	1955769,1	4230,9

### Conclusions

1. The gas dynamics of turboimpact separators of multiphase mixtures of high-pressure fuels was investigated.

2. The optimal design of a turboimpact separator with a radial arrangement of a coagulation element with

a flow rate of 43.7 m/s was obtained, which contributes to turboimpact particle transfer.

3. It was established that the optimal pressure drop of 1 KPA is observed in a turboimpact separator with a radial arrangement of a coagulation element, which allows using this design for cleaning multiphase mixtures of high-pressure fuels.

### References

1. Calvert, S. and Englund, G. M. (1988). Protection of the atmosphere from industrial pollution. Handbook. Moscow: Metallurgiya. Part 1. 760.
2. Calvert, S. and Englund, G. M. (1988). Protection of the atmosphere from industrial pollution. Reference book. Moscow: Metallurgy. Part 2. 770.
3. Ryzhkov, S. S. (2006). Thermophoretic deposition of liquid particles of turbulent gas flow. National Academy of Sciences of Ukraine, Institute of Technical Thermophysics. Kyiv, 208.
4. Ryzhkov, S. S., Serbin, S. I., Bilyk, B. I. (2005). Development of a generalized mathematical model of the processes of turbophoretic transfer of particles in a highly turbulized flow. *4th International. scientific-technical conf. "Problems of ecology and energy saving in shipbuilding"*. Nikolaev. P. 256–258.
5. Ryzhkov, A. S. (2004). Investigation of aerosol capture in non-isothermal hydrodynamic coagulators of the Venturi pipe type. *Industrial Heat Engineering*, 26, 6, 65–69.

6. Ryzhkov, A. S. (2005). Experimental studies of the hydrodynamic coagulator of the oil separator. *Mater. 4th International. scientific-technical conf. "Problems of ecology and energy saving in shipbuilding"*. Nikolaev. P. 171–172.
7. Ryzhkov, S. S., Basok, B. I. (2001). Ecological resource-saving technologies for industrial heat engineering based on dispersed two-phase media. *Industrial Heat Engineering*, 23 (4–5), 141–145.
8. Retrieved from <http://selton.com.ua>
9. Retrieved from <http://www.parker.com>
10. Retrieved from <http://www.ansys.com>
11. Basok, B. I., Ryzhkov, S. S., Bortsov, O. S. (2013). Investigation of the preliminary stage of the separator of multiphase mixtures of high-pressure fuels within the internal problem. *Industrial heat engineering*.

Received 28.03.2023

**Рижков Сергій**

Доктор технічних наук, професор, [orcid.org/0000-0001-9560-2765](https://orcid.org/0000-0001-9560-2765)

Політехнічний коледж Яньчен, Міжнародна академія морських наук, технологій та інновацій, Яньчен, Китай

**Ченжиан Донг**

<https://orcid.org/0000-0003-3529-6529>

Школа автомобільного транспорту, Яньченський політехнічний коледж, Яньчен, Китай

**ДОСЛІДЖЕННЯ ГАЗОДИНАМІКИ ВИСОКОЕФЕКТИВНОГО ТУРБОУДАРНОГО СТИСНЕНОГО  
ГАЗОДЕЛЯТОРА ДЛЯ ГАЗОТУРБІННОЇ УСТАНОВКИ**

**Анотація.** Досліджено газодинаміку багатofазних сумішей палив високого тиску в турбоімпатних сепараторах з коагуляційними конструктивними елементами при витраті робочого середовища  $G = 500 - 2200$  кг/год. Геометрія турбоімпатного сепаратора з радіальним напрямним струминним елементом складається з першого ступеня та сепаратора, що складається з пластини діаметром 250 мм, на діаметрі 97 мм якої розташований гофрований сепараційний елемент. Його розміри змінюються від 10 до 40 мм, залежно від робочої геометрії. У нижній частині першого ступеня сепаратора є канавки прямокутної форми  $3 \times 2$  мм на відстані 27 мм. У другому ступені сепаратора діаметром 270, 240 і 180 мм відповідно є наскрізні прямокутні канавки  $5 \times 10$  мм. У турбоударному сепараторі з радіальним коагуляційним елементом спостерігався рівномірний розподіл швидкостей, максимальна становить 43,7 м/с, що свідчить про рівномірний турбоударний перенос частинок. Турбоударний сепаратор з радіальним напрямним струминним елементом характеризується близьким розташуванням гофрованого сітчастого елемента до зони струминного очищення. Перед течією, в каналі передовий елемент сітки утворює вихрові зони, що в подальшому призведе до витіснення неосаджених частинок до нижньої стінки каналу. У турбоударному сепараторі першого ступеня очищення з елементом радіальної коагуляції після проходження робочого середовища зони струминного очищення потік рівномірно розподіляється по всій ділянці каналу, що сприяє рівномірному розподілу полідисперсної фази в робочій зоні (середній перед елементом сітки). Встановлено, що в турбоударному сепараторі з радіальним розташуванням коагуляційного елемента спостерігається оптимальний перепад тиску 1 кПа, що дає змогу використовувати цю конструкцію для очищення багатofазних сумішей палив високого тиску.

**Ключові слова:** турбоударний перенос; сепаратор; осадження частинок; газодинаміка; багатofазні суміші; паливо високого тиску

**Link to the publication**

APA Ryzhkov, Sergiy, & Chengjian, Dong, (2023). Research of gas dynamics of highly efficient turbo-impact compressed gas separator for gas turbine installation. *Management of Development of Complex Systems*, 53, 120–126, [dx.doi.org/10.32347/2412-9933.2023.53.120-126](https://doi.org/10.32347/2412-9933.2023.53.120-126).

ДСТУ Рижков С., Ченжиан Д. Дослідження газодинаміки високоєфективного турбоударного стисненого газоделятора для газотурбінної установки. *Управління розвитком складних систем*. Київ, 2023. № 53. С. 120 – 126, [dx.doi.org/10.32347/2412-9933.2023.53.120-126](https://doi.org/10.32347/2412-9933.2023.53.120-126).